Frontiers in Applied Physics, Materials Science and Nanotechnology
https://www.iahiservices.com

Research Article

Synthesis and Characterization of Rare-Earth-Doped Nanosilica from Rice Husk for Potential Luminescent Downshifting Applications in Photovoltaics

Mbakaan, Celestine[1*] https://orcid.org/0000-0001-8001-9788

Physics with Electronics Section, Department of Science Laboratory Technology, Benue State Polytechnic, Ugbokolo
Corresponding Author Email: celestinembakaan@gmail.com

Abstract- The limited UV–visible photon harvesting capability of silicon solar cells motivates the development of luminescent down-shifting (LDS) materials capable of converting high-energy photons into wavelengths more effectively absorbed by Si. In this study, high-purity nanosilica extracted from five rice cultivars was doped with Dy^{3+}, Eu^{3+}, and Sm^{3+} to evaluate its suitability as a sustainable LDS material and benchmarked against TEOS-derived silica. The RH-derived silica exhibited high surface areas (>200 $m^2 \cdot g^{-1}$) and nanoscale particle sizes (14–70 nm), enabling efficient dopant dispersion and enhanced optical interactions. Bandgap analyses revealed dopant-induced narrowing from ~5.7 eV to ~4.5 eV, confirming the introduction of energy levels that facilitate UV absorption and radiative recombination in the visible region. Photoluminescence measurements further demonstrated strong spectral conversion: Dy^{3+}-doped samples produced blue–yellow emissions capable of near-white output (CCT 4,000–6,256 K), Eu^{3+}-doped silica displayed intense red emission dominated by the hypersensitive $^5D_0 \rightarrow {}^7F_2$ transition (CIE x = 0.627, y = 0.367), and Sm^{3+}-doped samples generated tunable orange–red luminescence with concentration-dependent quenching. These emissions align closely with the external quantum efficiency (EQE) peak of Si (~450–650 nm), confirming their usefulness for LDS. Comparative optical studies showed that RH-derived phosphors perform as well as or better than TEOS-derived analogues, driven by defect-assisted sensitization and the highly porous silica network. These synergistic properties validate RE-doped RH nanosilica as a cost-effective, sustainable, and high-performing LDS material capable of enhancing silicon solar-cell spectral utilization, while demonstrating a viable pathway for converting agricultural waste into high-value photonic materials.

Article Key Information

Keywords: Luminescent downshifting (LDS); Rare-earth-doped nanosilica; Rice husk valorization; Photoluminescence and chromaticity tuning; Waste-to-wealth nanomaterials; Photovoltaic spectral management

Received: 20th July 2025 **Revised:** 25th October 2025 **Accepted**: 18th November 2025 **Published**: 27th November 2025

1. Introduction

The global demand for clean and sustainable energy sources has intensified over the last few decades due to growing concerns about climate change, energy insecurity, and environmental degradation [1]. Solar photovoltaic (PV) technology is considered one of the most promising alternatives to fossil fuels because of its abundance, renewability, and scalability [2]. However, despite remarkable progress, the efficiency of commercial PV modules

remains constrained by inherent optical losses. One major limitation is the mismatch between the solar spectrum and the absorption profile of conventional silicon-based solar cells, which are unable to effectively harvest high-energy ultraviolet (UV) photons [3]. This spectral mismatch results in thermalization losses, where excess photon energy is dissipated as heat rather than converted into useful electricity.

Luminescent downshifting (LDS) materials have emerged as a viable strategy to address this challenge [4]. LDS involves the absorption of high-energy photons followed by re-emission at longer wavelengths better matched to the bandgap of the solar cell [5]. By converting UV light into visible wavelengths, LDS materials enhance the overall spectral utilization, improve power conversion efficiency, and reduce photo-degradation of solar modules [6]. A central requirement for effective LDS materials is the integration of highly stable host matrices with rare-earth (RE) activator ions that exhibit sharp, intense, and tunable emission bands [7].

Silica (SiO_2)-based matrices have gained considerable attention as hosts for luminescent centers because of their chemical stability, wide bandgap, and excellent transparency [8]. In particular, nanosilica offers enhanced surface area, tunable porosity, and unique size-dependent optical properties, which are beneficial for incorporating RE dopants [9]. However, conventional methods for synthesizing nanosilica often rely on expensive precursors such as tetraethyl orthosilicate (TEOS) and other alkoxysilanes, which significantly limit scalability [10]. In the context of developing countries, where resource optimization and sustainable innovation are paramount, the search for low-cost, renewable precursors for silica is of both scientific and socio-economic significance.

Rice husk (RH), an abundant agro-industrial byproduct, represents one of the most promising biomass-derived sources of silica [11]. Globally, rice production generates millions of tons of husks annually, of which a substantial fraction is either openly burned or disposed into landfills, causing severe environmental and health challenges including air pollution, greenhouse gas emissions, and vector proliferation [12]. Importantly, rice husk contains 15–28 wt% amorphous silica embedded in its lignocellulosic matrix [13]. When subjected to controlled thermal or chemical treatment, rice husk can yield high-purity nanosilica suitable for advanced material applications [14]. This valorization pathway not only mitigates waste management concerns but also aligns with the global agenda of “waste-to-wealth” transformation, a key component of circular economy frameworks [15].

Rare-earth doping of rice-husk-derived nanosilica further expands its application potential in luminescent technologies. RE ions such as Eu^{3+}, Sm^{3+}, Dy^{3+}, and Tb^{3+} exhibit characteristic f–f transitions, producing sharp emission lines across the visible spectrum [16]. Their electronic configurations are shielded by filled $5s^2$ and $5p^6$ orbitals, which minimize the influence of the surrounding host matrix and result in high color purity and thermal stability [17]. When incorporated into nanosilica, these ions can act as efficient luminescent centers for LDS applications, enabling the conversion of high-energy UV photons into longer-wavelength emissions compatible with silicon solar cells [18]. Moreover, the ability to tune emission colors through selective RE doping provides flexibility in designing composite LDS layers tailored to specific photovoltaic architectures [19].

The utilization of rice husk for the synthesis of RE-doped nanosilica thus presents a multifaceted innovation with socio-economic, environmental, and technological implications. From a socio-economic standpoint, the approach creates value from agricultural waste, potentially stimulating rural economies in rice-producing regions [20]. Environmentally, it offers a sustainable waste management strategy, reducing carbon emissions from husk burning and minimizing landfill burdens [21]. Technologically, it contributes to next-generation PV systems by addressing spectral mismatch losses, thereby improving energy yield and advancing the transition toward clean energy futures [22].

Previous studies have demonstrated the feasibility of extracting silica from RH using acid leaching followed by controlled calcination [23]. High-purity amorphous nanosilica can be obtained at moderate processing temperatures (500–700 °C), with properties comparable to those derived from synthetic precursors [24]. Researchers have further shown that RE-doped silica nanostructures exhibit strong photoluminescence under UV excitation, confirming their potential in optoelectronic applications [25]. However, studies specifically targeting the synthesis and characterization of RE-doped nanosilica from rice husk for LDS in photovoltaics remain limited. The intersection of waste valorization, rare-earth luminescence, and solar energy conversion therefore represents an underexplored yet highly promising research frontier.

This study is designed to synthesize nanosilica from rice husk, dope it with selected RE ions, and evaluate its structural, morphological, and photoluminescent properties. By establishing a systematic correlation between processing conditions, dopant incorporation, and optical performance, the research aims to develop a sustainable class of LDS materials tailored for photovoltaic enhancement.

2.0 Review of Literature

2.1 Overview of Luminescent Downshifting (LDS) in Photovoltaics

Luminescent downshifting (LDS) represents a pivotal strategy for overcoming optical losses in photovoltaic (PV) devices by converting high-energy ultraviolet (UV) photons into lower-energy visible emissions that better match the absorption profile of silicon-based solar cells. The fundamental principle involves photon absorption by a luminescent center, followed by re-emission at longer wavelengths with minimal thermalization losses [26], [27]. This process enhances the spectral response and stability of PV modules by mitigating UV-induced degradation while improving overall power conversion efficiency [28], [1], [3].

The integration of LDS materials as surface coatings or interlayers in PV systems has been widely explored, with rare-earth (RE) doped phosphors emerging as some of the most promising candidates due to their sharp emission lines, high quantum efficiencies, and excellent photostability [29], [30]. Such materials serve dual functions—improving device efficiency and extending operational lifetime by spectral management and optical protection mechanisms [28], [3].

2.2 Silica as a Host Matrix for Luminescent Materials

Silica (SiO_2) has long been recognized as an excellent host matrix for luminescent dopants owing to its wide bandgap, chemical inertness, and optical transparency [31], [32]. At the nanoscale, silica exhibits enhanced surface area and tunable porosity, which facilitate efficient dopant incorporation and minimize non-radiative decay processes [33], [34]. The amorphous nature of silica further ensures homogeneous dopant distribution and prevents concentration quenching often observed in crystalline hosts [35], [36].

Studies have shown that defect-related centers such as oxygen-deficiency centers (ODCs) and non-bridging oxygen hole centers (NBOHCs) contribute to intrinsic luminescence in silica nanoparticles [37], [38], [39]. These defect-induced emissions can be tuned by synthesis conditions, such as calcination temperature and precursor composition, to yield blue to green photoluminescence [40]. The combination of defect engineering and RE doping thus provides a versatile platform for designing broad- and narrow-band emitters suitable for optical applications ranging from solid-state lighting to photovoltaics [36].

2.3 Rice Husk as a Sustainable Source of Silica

Rice husk (RH), an abundant agro-industrial byproduct, contains between 15–28 wt% amorphous silica embedded in a lignocellulosic framework [41]. Owing to its high silica content and renewable nature, RH has been increasingly recognized as a sustainable precursor for nanosilica production [42], [43], [44]. When properly treated, it yields amorphous, high-purity silica comparable to synthetic sources such as tetraethyl orthosilicate (TEOS) [45], [46].

Globally, open burning or indiscriminate disposal of rice husk has contributed to environmental degradation, releasing carbon dioxide, particulates, and greenhouse gases [43]. The transformation of this biomass waste into value-added nanomaterials therefore supports both environmental remediation and sustainable materials development [44], [47], [48].

Wang et al. [43], [41], [49] demonstrated that controlled acid leaching followed by calcination between 500–700 °C effectively removes metallic impurities and yields amorphous silica nanoparticles. Similarly, Bhagiyalakshmi et al. [47], [50] reported that dual-acid pretreatment with HCl and H_3PO_4 enhances silica purity and stabilizes the amorphous phase through P–O–Si bond formation. The specific surface area of RH-derived silica (up to 219 m^2/g)

has been shown to exceed that of commercial silica, conferring superior textural properties for catalytic and luminescent applications [51].

2.4 Synthesis and Processing Approaches for Rice-Husk-Derived Nanosilica

The synthesis of nanosilica from rice husk typically involves acid leaching to remove alkali and alkaline-earth impurities, followed by thermal decomposition (calcination) to convert the organic matrix into silica ash [52], [53]. Process parameters—including acid concentration, calcination temperature, and heating rate—strongly influence the purity, particle size, and amorphous character of the resulting silica [54], [55].

Bhagiyalakshmi et al. [47], [50] optimized dual-acid (HCl/H_3PO_4) pretreatments to minimize residual carbon and metallic impurities, while Wang et al. [41], [43] employed controlled calcination to produce highly active amorphous silica frameworks. The resulting silica nanoparticles exhibit superior textural and adsorption properties due to the development of mesoporous networks [33], [51].

Recent works by Bansal et al. [56] and Habeeb and Fayyadh [32] have also confirmed that processing conditions significantly affect silica morphology and optical activity. Smaller particle sizes obtained through optimized calcination enhance surface reactivity and dopant dispersion, which are critical for efficient luminescent performance [57].

2.5 Rare-Earth (RE) Doping and Photoluminescence in Silica Systems

The incorporation of rare-earth ions into silica matrices has revolutionized luminescent materials design, owing to the shielded 4f electronic configuration of RE elements such as Eu^{3+}, Dy^{3+}, Sm^{3+}, and Tb^{3+}, which produce sharp, color-pure emissions across the visible spectrum [33], [34], [45]. The characteristic f–f transitions are minimally affected by the host lattice, yielding thermally stable emissions with narrow linewidths and high color purity [29], [30].

Eu^{3+}-doped silica systems exhibit intense red emissions ($^5D_0 \rightarrow {}^7F_2$ transitions), often associated with asymmetry in the local environment of Eu^{3+} ions [46], [30]. Dy^{3+} ions emit dual bands at ~480 nm (blue) and ~575 nm (yellow), whose combination yields near-white light suitable for broadband LDS and solid-state lighting [29]. Sm^{3+}-doped systems display tunable orange–red emission depending on dopant concentration and host symmetry, although excessive doping may lead to concentration quenching [58].

Several studies have confirmed that RE incorporation into silica hosts can narrow the optical bandgap (from ~5.7 to ~4.5 eV), creating intermediate energy levels that enhance UV absorption and emission efficiency [40]. The synergistic interplay between intrinsic defect states and RE dopants underlies the superior photoluminescent performance of such hybrid systems [35], [36].

2.6 Rice-Husk-Derived RE-Doped Nanosilica: Advances and Prospects

The valorization of rice husk into RE-doped nanosilica represents a confluence of green chemistry, materials innovation, and renewable energy research [28], [56], [47]. By transforming agricultural residues into optically functional materials, researchers have demonstrated that waste-derived nanosilica can exhibit luminescent properties equal or superior to those obtained from synthetic precursors [59]. The amorphous structure, high surface area, and presence of defect states in RH-derived silica enhance dopant dispersion and energy transfer efficiency, leading to stronger and broader emissions [51], [36].

Wei et al. [59] and Wang et al. [28] reported that RH-based luminescent materials display strong blue–green or red emissions under UV excitation, confirming their potential for LDS coatings in photovoltaic modules. Moreover, the spectral tunability achieved through Dy^{3+}, Eu^{3+}, and Sm^{3+} doping makes these materials ideal for customizing emission profiles to match solar cell band gaps [29], [30], [52].

In comparison to TEOS-derived silica, RH-based systems offer cost and environmental advantages without compromising optical quality [43], [31]. Their successful synthesis validates the waste-to-wealth paradigm and supports the integration of circular economy principles in advanced materials science [44], [56], [47].

2.7 Knowledge Gaps and Research Direction

Although numerous studies have explored either RH-derived silica synthesis or RE-doped photoluminescent systems individually, there remains limited research that combines both aspects for LDS in photovoltaics [28], [52]. The systematic relationship between rice cultivar composition, synthesis route, dopant incorporation, and optical performance remains poorly understood. In particular, quantitative correlations between surface area, defect density, and photoluminescence intensity have not been fully established.

Furthermore, while laboratory-scale demonstrations have confirmed emission tunability and efficiency enhancement, real-world device integration and spectral conversion efficiency measurements are scarcely reported [52], [53]. Addressing these gaps requires a comprehensive characterization of structural, morphological, and optical parameters to establish design guidelines for high-performance LDS nanophosphors derived from renewable precursors.

3.0 Materials and Methods

3.1. Materials and Reagents

Rice husk (RH), obtained as the primary raw material, was used as the silica precursor. Analytical reagent-grade acids, including hydrochloric acid (HCl, 37 wt%), nitric acid (HNO_3, 70–75 wt%), and phosphoric acid (H_3PO_4, 85 wt%) were procured from Sigma-Aldrich. Ethanol (99.9%, analytical grade), sodium hydroxide pellets, and ammonium hydroxide solution (NH_4OH) were obtained from Merck. Poly(vinylpolypyrrolidone) (PVP, Fluka) was employed as a capping agent to prevent agglomeration during synthesis. Tetraoctylammonium bromide (TOAB, $C_{32}H_{68}BrN$, Fluka) was used as a surfactant. Rare-earth precursors included dysprosium (III) nitrate hydrate (99.9%, trace-metal basis, Sigma-Aldrich), europium (III) nitrate pentahydrate (99.9%, Sigma-Aldrich), and samarium (III) nitrate hexahydrate (99.9%, Sigma-Aldrich). Tetraethylorthosilicate (TEOS, analytical grade, 99.9%, Merck) was employed as a comparative synthetic silica precursor. Deionized water from institutional laboratories was utilized throughout the experiments.

The choice of reagents and dopants was informed by prior reports establishing the effectiveness of lanthanide nitrates as activator ions for luminescent applications [23]–[25].

3.2. Instrumentation

The synthesis and characterization employed advanced laboratory facilities. Thermal decomposition and calcination were carried out in a programmable box furnace. Morphological and particle-size analyses were performed using scanning electron microscopy (SEM) and transmission electron microscopy (TEM). Structural characterization was achieved by X-ray diffraction (XRD), while surface chemistry was probed using Fourier-transform infrared spectroscopy (FTIR). Surface area and porosity were determined by nitrogen adsorption–desorption using the Brunauer–Emmett–Teller (BET) method on a Micromeritics TriStar II 3020 system [26]. Optical absorption spectra were recorded with a UV–Visible spectrophotometer, while photoluminescence (PL) studies were conducted using a spectrofluorometer equipped with a 365 nm UV excitation source.

The instrumentation suite was chosen to ensure that the structural, morphological, and photophysical characteristics of the nanosilica and RE-doped samples were rigorously established in line with best practices in luminescent nanomaterials research [27].

3.3. Software Tools

ImageJ software was employed to determine particle size distributions from TEM micrographs, while CIE colorimetry software was used to calculate chromaticity coordinates from photoluminescence data. OriginPro

software was utilized for data plotting, spectral deconvolution, and curve fitting. Such analytical tools are essential to provide a quantitative assessment of size distribution, emission characteristics, and chromaticity diagrams for LDS evaluation [28].

3.4. Rice Husk Collection and Preparation

Rice husks of five distinct cultivars commonly grown in North-Central Nigeria namely *Zemuje* (FARO-52), *Sipi* (FARO-44), *Mass* (Nerica-II), *Osi* (Nerica-I), and *Turn 2* (FARO-46)—were collected from the Wurukum Rice Milling Station, Makurdi, Benue State, Nigeria. All varieties belong to the *Oryza sativa* species. The selection of multiple cultivars was motivated by the hypothesis that silica yield and purity vary with genotype, as previously observed by Bryant et al. [8].

The husks were sieved using a 75 μm mesh to remove soil and extraneous matter, washed thoroughly with deionized water, and dried at ambient conditions for 24 h. This pretreatment ensured the reduction of extraneous impurities, which could otherwise affect the purity and structural properties of extracted nanosilica [29].

3.5. Synthesis of Nanosilica from Rice Husk

3.5.1 Acid Pretreatment and Calcination

Fifty grams of air-dried RH were refluxed with 200 mL of 10 wt% HCl for 2 h under constant stirring to remove metallic impurities, particularly potassium and calcium ions known to interfere with silica network formation [30]. The acid-treated husks were washed repeatedly with deionized water until a neutral pH was achieved and subsequently dried at 110 °C for 24 h.

Calcination was performed at 550 °C for 6 h with a heating rate of 10 °C/min. This condition was selected to achieve amorphous silica while preventing excessive carbon burnout, which has been shown to introduce photoluminescent defect centers [31]. The resulting ash was ground to fine powder, yielding amorphous nanosilica.

3.5.2. Dual-Acid Pretreatment (HCl/H_3PO_4)

In a modified route, RH samples pretreated with HCl were further soaked in 0.8 M H_3PO_4 before calcination. This dual-acid pretreatment was optimized to enhance silica yield and reduce residual impurities, building upon reports that phosphoric acid improves silica stability and optical purity [32].

3.6. Rare-Earth Doping of Nanosilica

RE doping was conducted via wet impregnation and sol-gel methods. For the impregnation route, predetermined molar ratios (0.01–0.10 M) of Eu^{3+}, Sm^{3+}, and Dy^{3+} nitrates were dissolved in ethanol–water mixtures and introduced to silica dispersions under vigorous stirring. The mixtures were aged for 12 h, dried at 100 °C, and annealed at 500 °C for 3 h to activate the luminescent centers. In parallel, sol-gel synthesis with TEOS was performed to benchmark the performance of RH-derived silica against conventional synthetic precursors [33].

3.7. Characterization of Doped Samples

The doped nanosilica samples were subjected to XRD, FTIR, SEM, and TEM analyses to confirm phase composition, functional groups, morphology, and size distribution. Photoluminescence studies were performed under UV excitation to evaluate emission intensity, spectral position, and chromaticity coordinates. BET analysis was employed to assess surface area, which influences dopant dispersion and emission properties.

This multi-technique characterization strategy ensured a robust evaluation of the suitability of RH-derived RE-doped nanosilica as luminescent downshifting materials for photovoltaics [34], [35].

4.0 Results and Discussion

4.1. Structural Properties of Undoped and Rare-Earth-Doped Nanosilica

The structural evolution of nanosilica derived from rice husk (RH-SiO_2) was investigated by X-ray diffraction (XRD). Figure 1 displays the diffraction patterns of RH-SiO_2 obtained from five rice cultivars (*Mass, Zemuje, Osi, Sipi,* and *Turn2*). All samples revealed a broad halo centered at $2\theta \approx 22.1°$, characteristic of amorphous silica [36], [37]. However, the RH-SiO_2–Zemuje sample exhibited additional sharp peaks indexed to the quartz phase (JCPDS card no. 79-1910), signifying partial crystallinity. This varietal dependence suggests that inherent compositional differences, particularly alkali metal content, can significantly influence the degree of structural ordering during calcination [38].

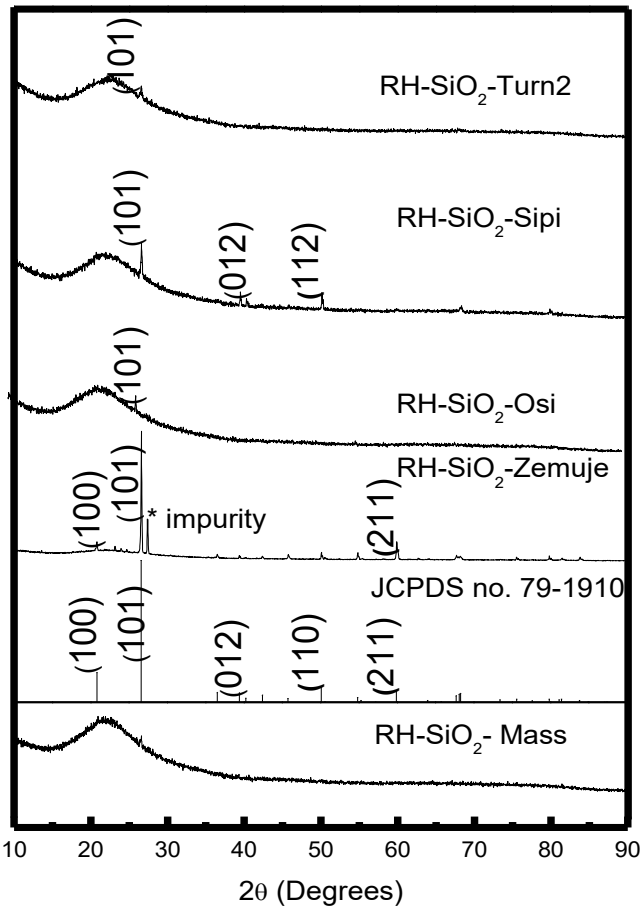

Figure 1: Diffraction patterns of RH-SiO_2 obtained from five rice cultivars

Further modification with dual-acid pretreatment (HCl/H_3PO_4), as shown in Figure 2, indicates that a high phosphoric acid concentration (≥0.8 M) suppresses crystallinity, yielding predominantly amorphous silica. This is consistent with prior reports that phosphorus enhances glass network stability by forming P–O–Si bonds, thereby retarding crystallization [39].

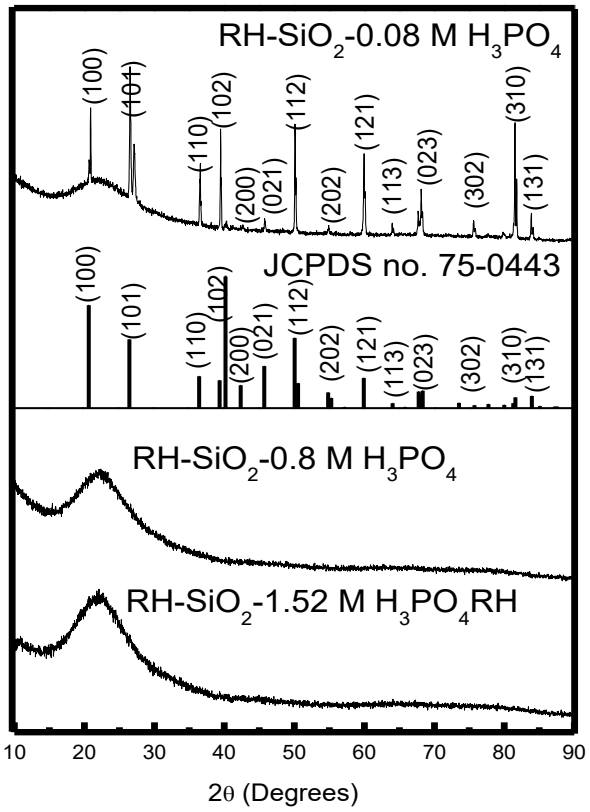

Fig 2: XRD patterns of RH-SiO_2 nanoparticles pretreated with HCl and soaked in different concentrations of H_3PO_4.

For rare-earth (RE) doping, the host RH-SiO_2 remained largely amorphous, but increasing dopant concentration of Eu^{3+} (1–3 mol%) induced the emergence of weak diffraction peaks at $2\theta = 21.6°$ (Figure 3), indexed to hexagonal silica (JCPDS card no. 33-1161).

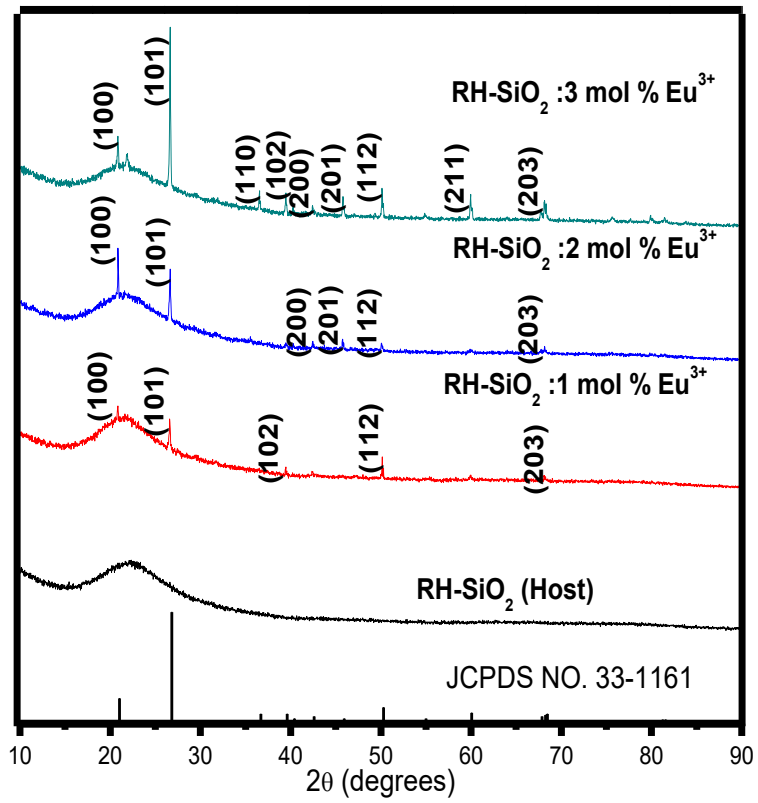

Fig 3: XRD patterns of RH-SiO_2: xEu^{3+} (x= 1, 2 and 3 mol %)

A similar amorphous-to-partial-crystalline transition was noted for Dy^{3+}- and Sm^{3+}-doped samples (Figures 4 and 5). The absence of RE-related secondary phases in all patterns suggests homogeneous incorporation of dopants into the silica matrix without clustering or segregation, a desirable condition for photonic applications [40], [41].

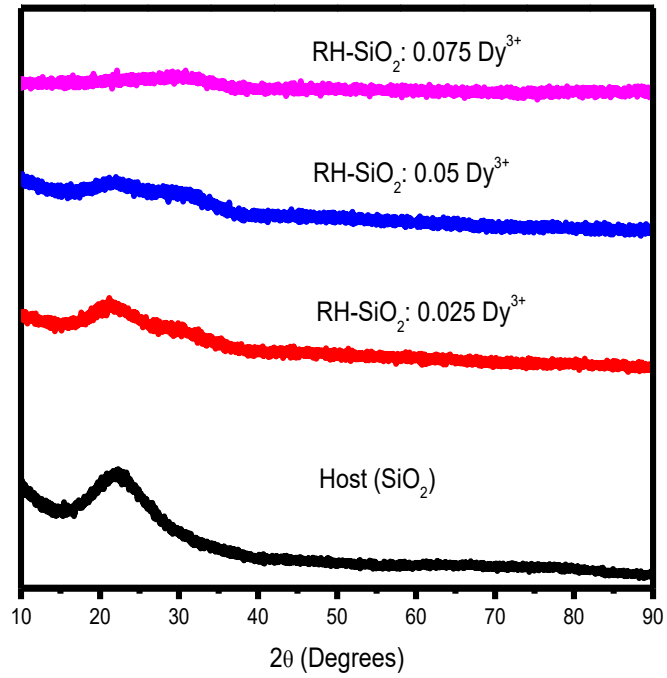

Fig 4: XRD result of RH-SiO_2 doped with different concentrations of dysprosium ions (RH-SiO_2: xDy^{3+} where x=0.025, 0.05 and 0.075 molar ratios)

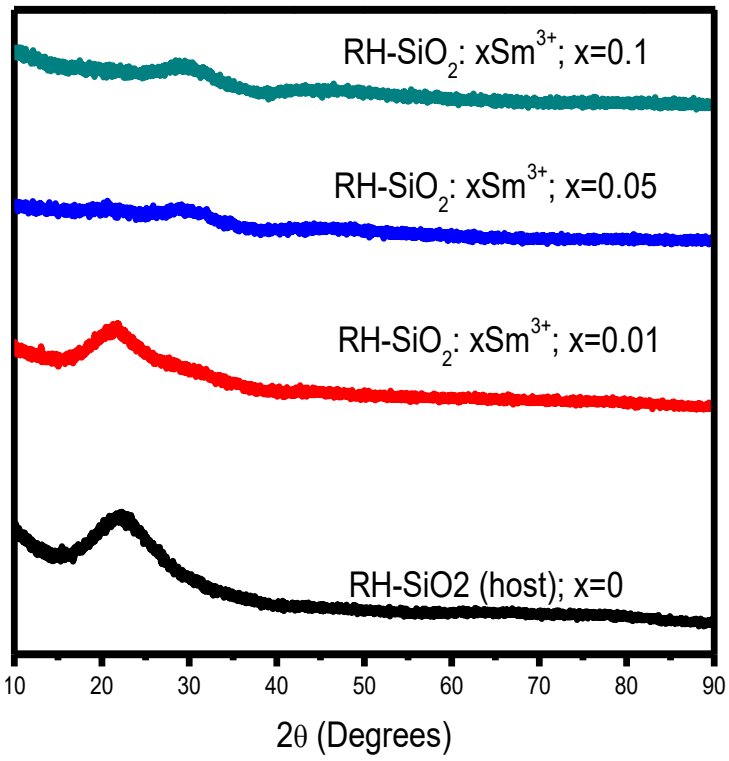

Fig 5: XRD result of RH-SiO_2 doped with different concentrations of samarium ions (RHS: xSm^{3+}; x=0.01, 0.05. and 0.1 molar ratios).

4.2. Morphology and Chemical Composition

SEM and TEM analyses revealed that undoped RH-SiO_2 consisted of agglomerated spherical nanoparticles with average diameters of 30–70 nm (Figures 6a–e, 7a–b). Upon doping with RE ions, particle morphology remained spherical, but average size decreased with higher dopant concentrations due to enhanced nucleation and growth restriction by ionic incorporation [42]. For instance, TEM analysis of RH-SiO_2:0.075Dy^{3+} yielded particle sizes averaging 14 nm (Figure 7c-d), while RH-SiO_2:3 mol% Eu^{3+} averaged 35 nm (Figure 8b).

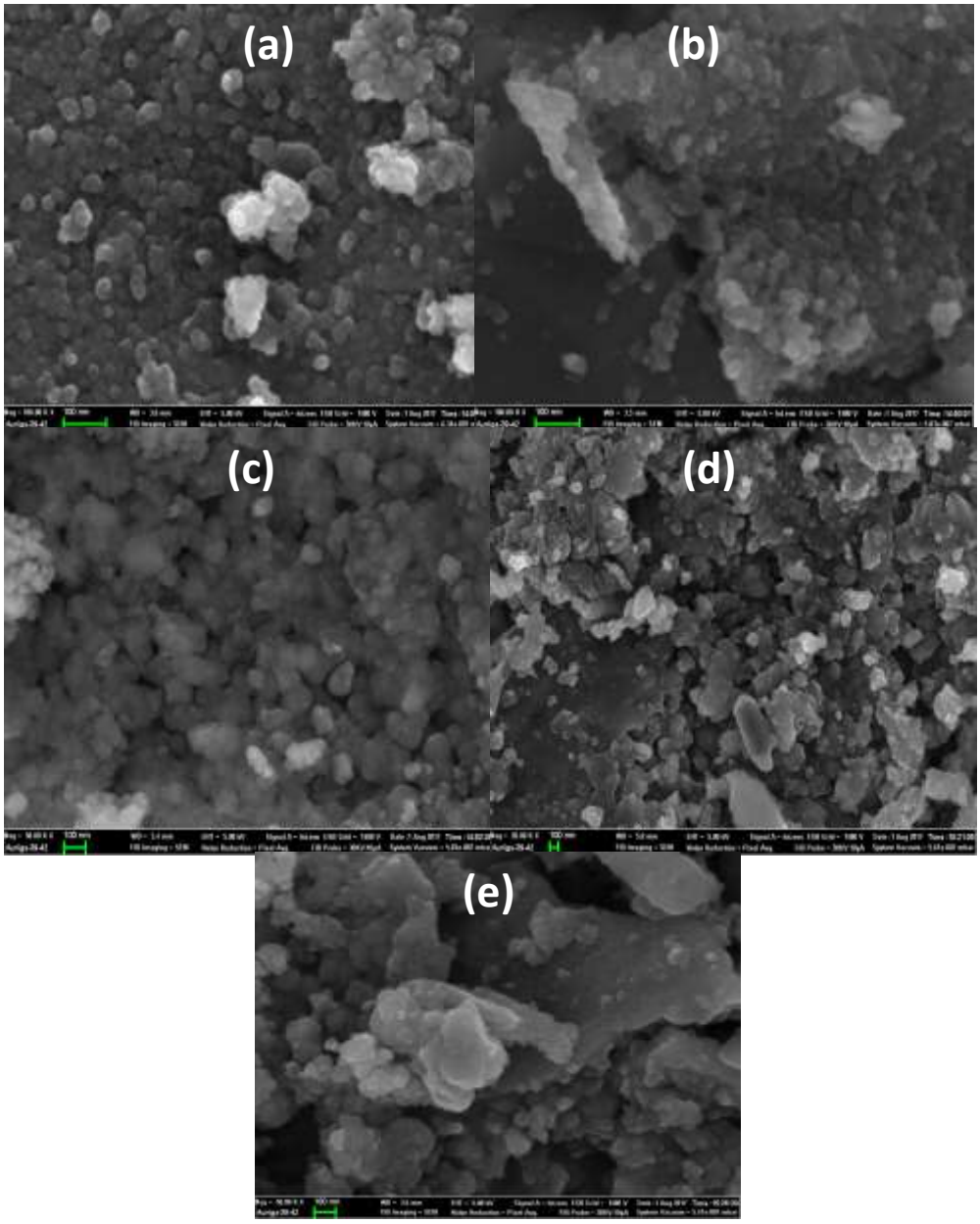

Fig 6: FESEM images of RH-SiO_2 derived from (a) Mass (b) Zemuje (c) Osi (d) Sipi and (e) Turn2 varieties.

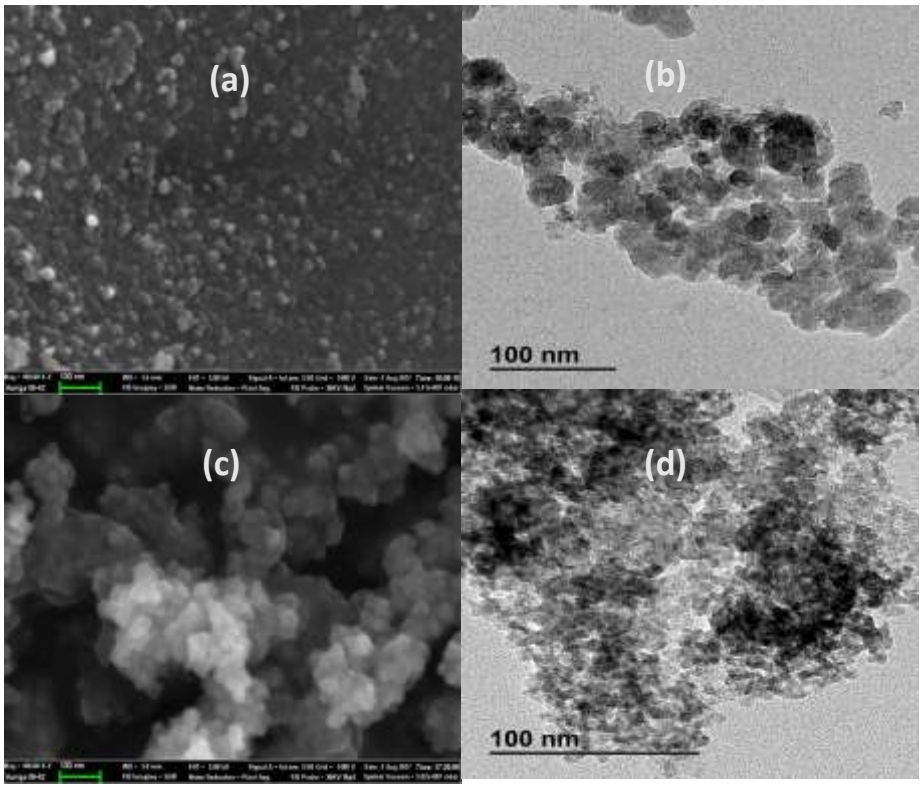

Figure 7: SEM (a) &TEM (b) images of RH-SiO_2 (host), and SEM (c) & TEM (d) images of RH-SiO_2: 0.075 Dy^{3+} nanophosphors

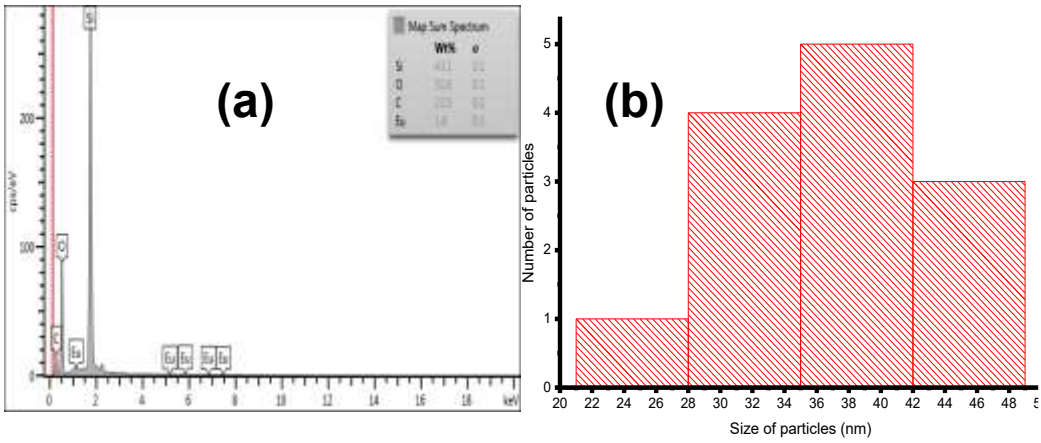

Fig 8: (a) SEM image, (b) EDX, (c) TEM image and (d) Histogram of RH-SiO_2: Eu^{3+} at 3 mol % samples

Energy dispersive X-ray spectroscopy (EDX, Figures 9a–b and 8a) confirmed the elemental composition of Si, O, and trace C in all samples, with clear detection of Eu and Dy signals in doped systems. The carbon peaks were attributed to residual biomass carbon or the carbon tape used during mounting [43]. These findings confirm successful incorporation of RE dopants into RH-derived nanosilica without significant impurity phases.

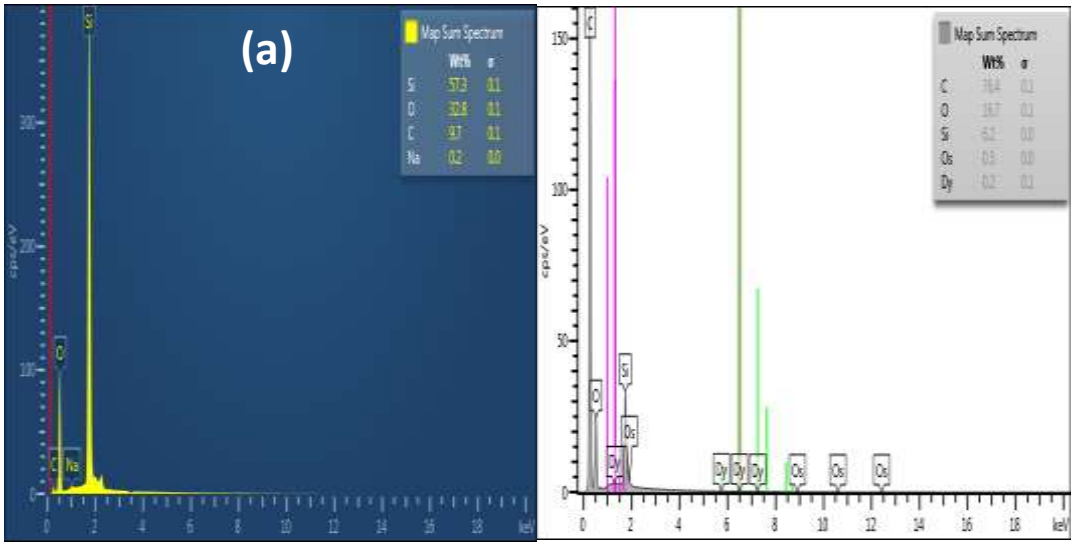

Fig 9: EDX spectra; RH-SiO_2 (host) (b) and RH-SiO_2: 0.075 Dy^{3+} nanophosphors

4.3 Surface Area and Porosity

BET nitrogen adsorption–desorption isotherms (Figure 10) revealed type IV isotherms with H3 hysteresis loops, typical of mesoporous materials. Surface areas of undoped RH-SiO_2 reached 219.1 m^2/g, substantially higher than commercial silica (53.8 m^2/g). Upon Eu^{3+} doping (3 mol%), surface area decreased slightly to 189.6 m^2/g, consistent with densification induced by increased structural ordering [44]. Such high surface areas are advantageous for homogeneous dopant dispersion, minimizing non-radiative centers, and enhancing luminescent performance [45].

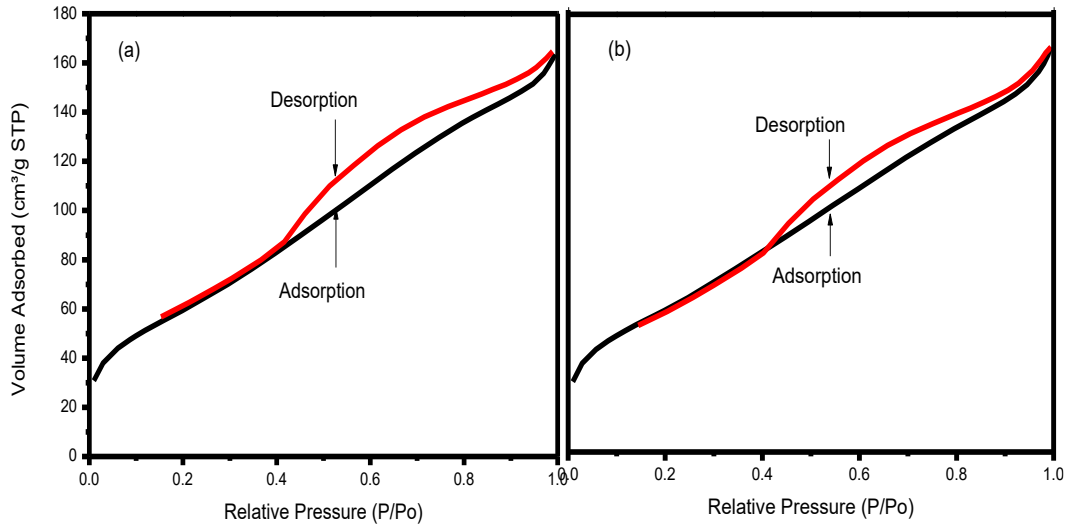

Fig. 10: N_2 adsorption-desorption isotherm of (a) RH-SiO_2 (host) and (b) RH-SiO_2: Eu at 3 mol %

4.4 Optical Absorption and Bandgap

Diffuse reflectance spectra (DRS, Figures 11a and 12a) of undoped RH-SiO_2 exhibited absorption features at 218–250 nm (band-to-band transitions) and 318–475 nm (defect-related absorptions).

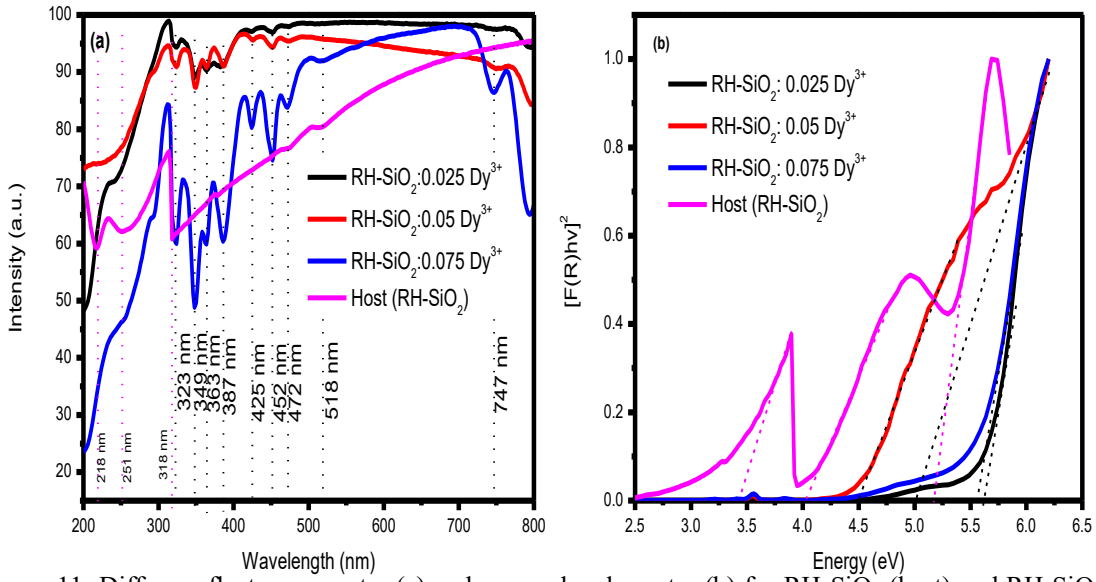

Figure 11: Diffuse reflectance spectra (a) and energy band spectra (b) for RH-SiO_2 (host) and RH-SiO_2: xDy^{3+} (x= 0.025, 0.05, and 0.075 Molar ratios) nanophosphors

RE-doped samples showed modified absorption profiles; for instance, Eu^{3+}-doped silica displayed a dominant absorption at 228 nm, while Dy^{3+}-doped samples introduced an additional peak at 30.2° in XRD linked to local bonding variations. Tauc plots (Figures 11b, 12b) revealed optical bandgaps ranging from 3.9–5.7 eV for undoped silica, narrowing to ~4.5 eV upon doping, indicating dopant-induced electronic states within the silica bandgap [46].

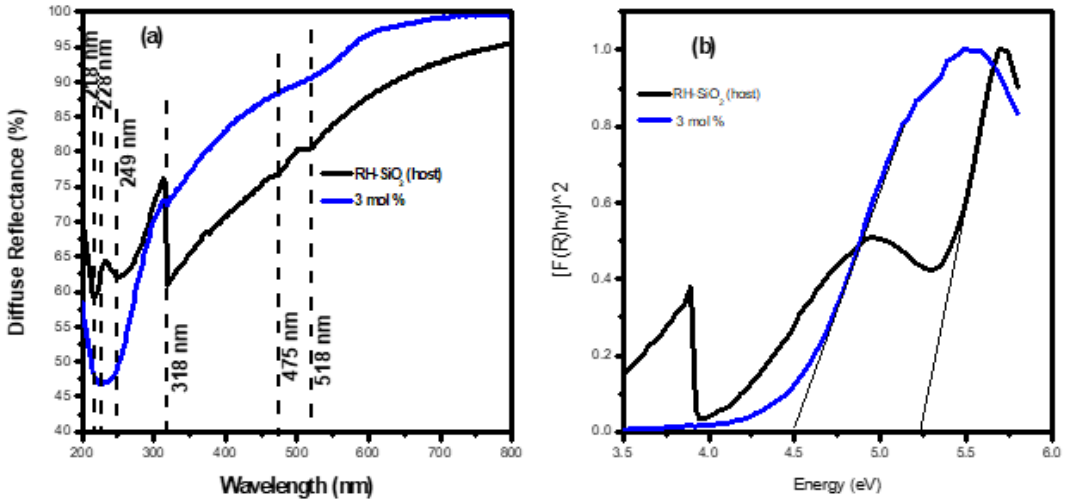

Figure 12: (a) Diffuse reflectance spectra and (b) energy band gaps of RH-SiO_2: xEu^{3+} (x= 3 mol %)

4.5 Photoluminescence (PL) Properties

4.5.1 Undoped RH-SiO_2

PL spectra (Figures 13) of undoped RH-SiO_2 exhibited multi-band emissions at 403–520 nm, attributed to oxygen-deficiency centers (ODCs), non-bridging oxygen hole centers (NBOHCs), and residual carbon-related centers [47], [48].

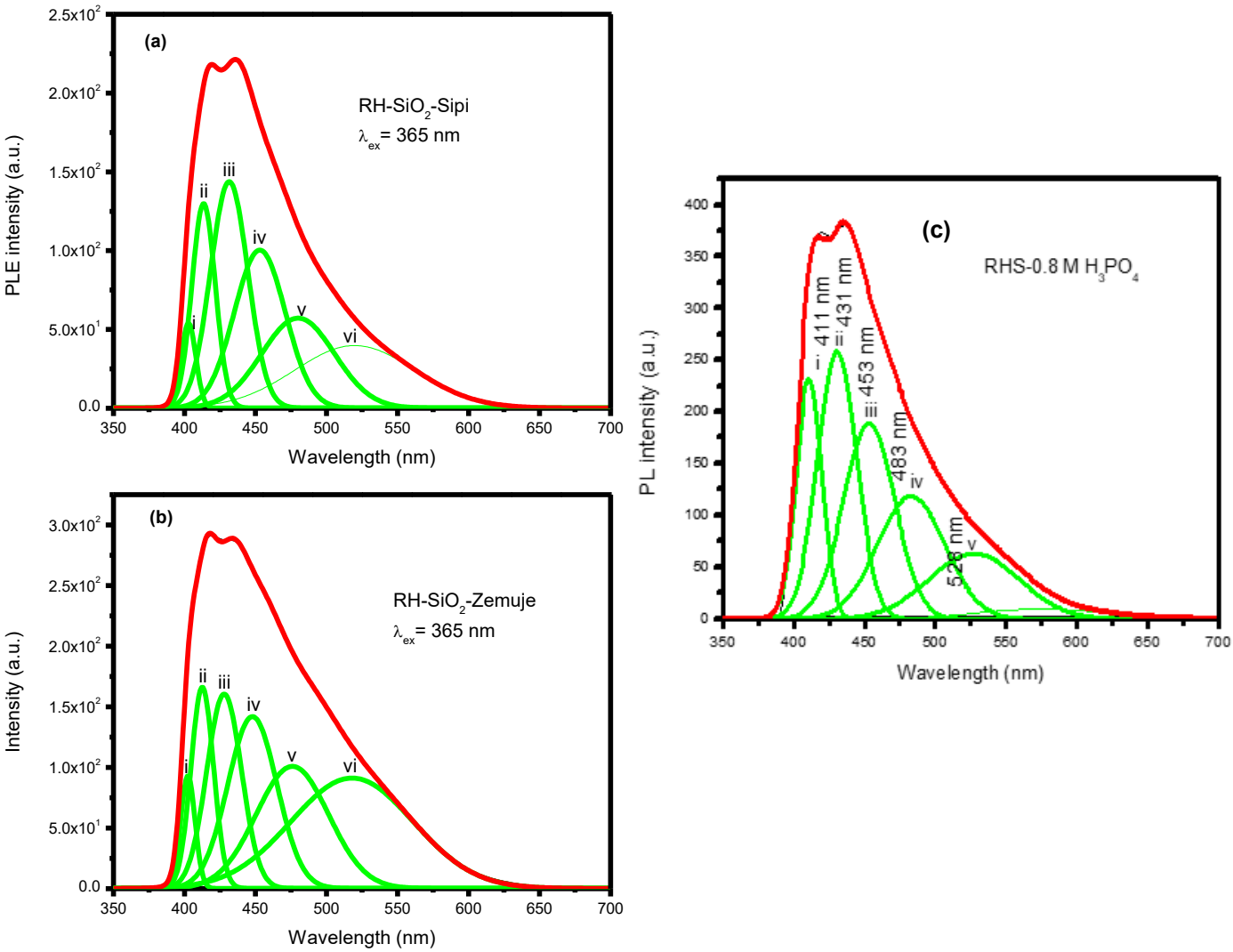

Fig 13: (a), (b) Deconvoluted Gaussian peaks of RH-SiO_2 samples excited at a wavelength of 365 nm (c) Deconvoluted Gaussian peaks of PL spectrum of RH-SiO_2-0.8 M H3PO_4 excited at 365 nm.

Emissions covered the blue–green region, with CIE coordinates shifting from deep-blue to sky-blue depending on rice variety (Table 1).

Table 1: CIE coordinates of RH-SiO_2 nanoparticles from RH of different Varieties

Sample	CIE coordinates	
	X	y
RH-SiO_2-Mass	0.1746	0.1861
RH-SiO_2-Zemuje	0.1738	0.1782
RH-SiO_2-Osi	0.1749	0.1865
RH-SiO_2-Sipi	0.1663	0.1360
RH-SiO_2-Turn2	0.1644	0.1425

4.5.2 Dy^{3+}-Doped RH-SiO_2

Dy^{3+}-doped samples exhibited intense emissions at ~480 nm ($^4F9/2 \rightarrow {}^6H15/2$, blue), 575 nm ($^4F9/2 \rightarrow {}^6H13/2$, yellow), and 664 nm ($^4F9/2 \rightarrow {}^6H11/2$, red) under excitation at 275 and 350 nm (Figure 14). The simultaneous presence of blue and yellow bands yielded near-white light with correlated color temperature (CCT) values ranging 4000–6256 K (Table 2), suitable for both indoor and outdoor solid-state lighting [49]. This validates the role of Dy^{3+} as a white-emitting activator in silica hosts.

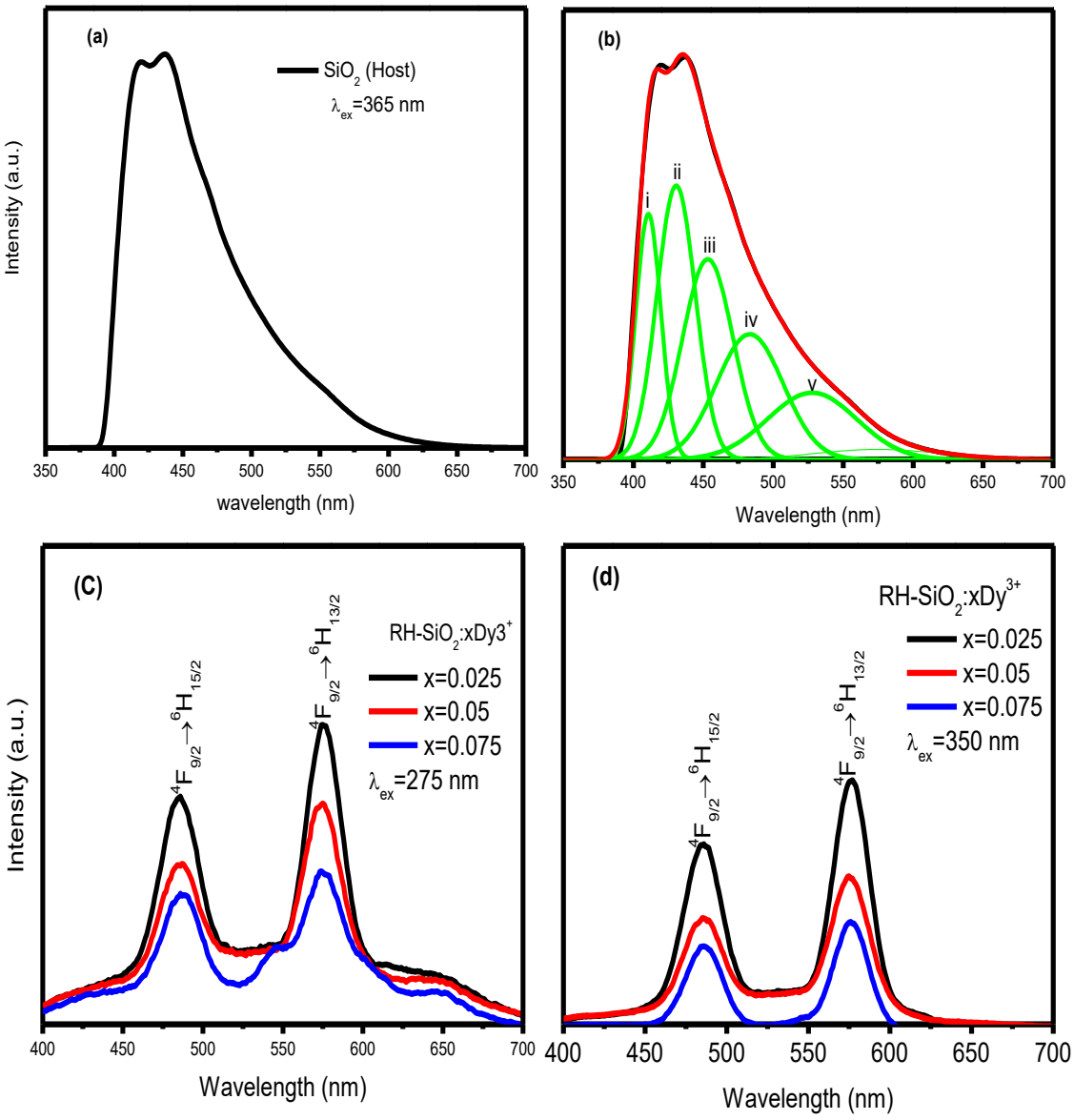

Fig 14: (a) Photoluminescence (PL) emission spectrum and (b) Deconvoluted bands of the host (RH-SiO_2) and Photoluminescence (PL) emission spectra of RH-SiO_2: xDy^{3+} (x = 0.025, 0.05 & 0.075 molar ratios) nanophosphors at (c) λ_{ex}= 275 nm and (d) λ_{ex}= 350 nm.

Table 2: CIE chromaticity coordinates, R_0 and CCT values of RH-SiO_2: Dy^{3+} nanophosphors

Sample RH-SiO₂ : x Dy³⁺	***CIE coordinates***		***Correlated color temperature (K)***	***R₀***
	x	y		
$\lambda_{ex} = 275nm$				
x = 0.025	0.3485	0.3992	5,020	1.34
x= 0.050	0.3460	0.4046	5,098	1.42
x= 0.075	0.3550	0.4139	4,868	1.16
$\lambda_{ex} = 350nm$				
x= 0.025	0.3472	0.4246	5,100	1.39
x= 0.050	0.3395	0.4249	5,318	1.44
x= 0.075	0.3053	0.4466	6,256	1.43

4.5.3 Eu^{3+}-Doped RH-SiO_2

Eu^{3+}-doped samples displayed sharp red emissions dominated by the $^5D0 \rightarrow {}^7F2$ transition at 617 nm, characteristic of forced electric dipole transitions (Figure 15).

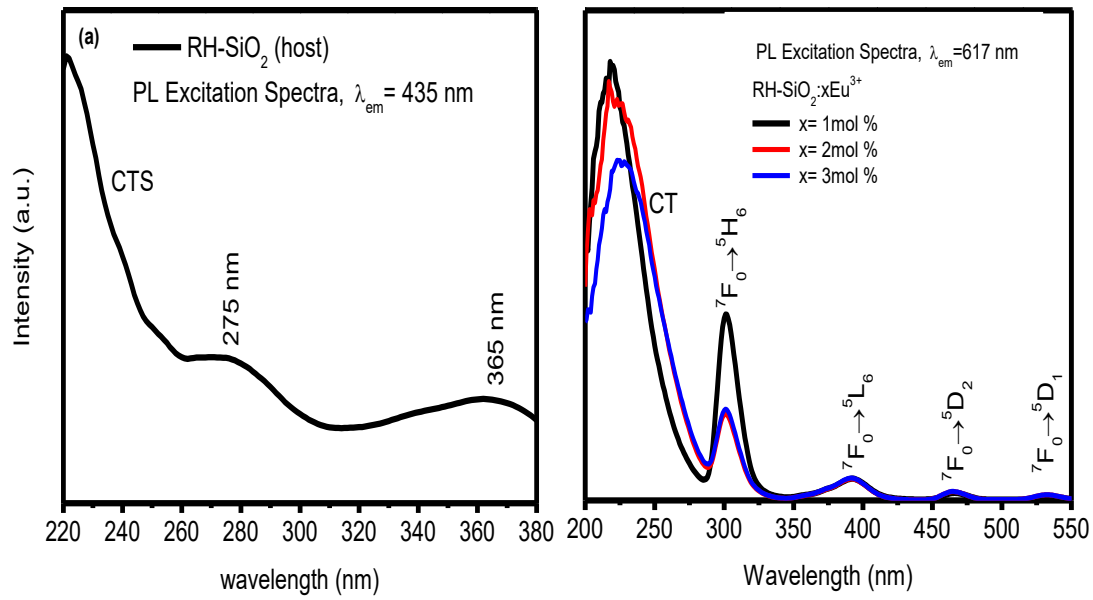

Fig 15: PL excitation spectra of (a) Host (RH-SiO_2) and (b) RH-SiO_2: xEu^{3+} (x = 1, 2 and 3 mol %

Judd–Ofelt analysis (Table 3) revealed asymmetry ratios (R > 1), indicative of distorted local environments around Eu^{3+} ions. CIE coordinates (x = 0.627, y = 0.367) closely matched NTSC standards for red phosphors, confirming suitability for display and photovoltaic downshifting applications [50].

Table 3: Calculated values of Judd-Ofelt parameters, asymmetry ratio, and radiative lifetime for RH-SiO_2: xEu^{3+}

Sample RH SiO_2 : x Eu^{3+}	Ω_2 $\times 10^{-20} cm^2$	Ω_4 $\times 10^{-20} cm^2$	R_0	τ_{rad} **ms**
$\lambda_{ex} = 393nm$				
x = 1 mol %	4.46	0.24	2.45	2.98
x = 2 mol %	5.23	0.20	3.01	2.56
x = 3 mol %	5.36	0.89	3.06	2.35
$\lambda_{ex} = 230nm$				
x = 1 mol %	4.01	0.16	2.73	3.34
x = 2 mol %	4.92	0.19	3.20	2.72
x = 3 mol %	5.00	0.14	3.28	2.69

4.5.4 Sm^{3+}-Doped RH-SiO_2

Sm^3-doped nanosilica exhibited concentration-dependent emission color tuning. At 0.01 M, red-orange emission dominated due to low activator density, shifting to yellow-orange at 0.05 M, and reverting to red-orange at 0.10 M due to concentration quenching (Table 4, Figures 16a–b).

Table 4: CIE Chromaticity Coordinates Values of RH-SiO_2: xSm^{3+} (x = 0.01, 0.05, 0.1 Molar Ratio) Nanophosphors

Sample RH-SiO_2 : x Sm^{3+}	***CIE coordinates***			
	x	y	x	y
	$\lambda_{ex} = 365nm$		$\lambda_{ex} = 400nm$	
x = 0.010	0.4710	0.5069	0.5170	0.4722
x= 0.050	0.3962	0.5610	0.4523	0.5186
x= 0.100	0.4894	0.4947	0.5143	0.4755

Such tunability highlights the role of activator concentration in controlling emission chromaticity [51].

4.5.5 Luminescent Downshifting (LDS) Potential

Collectively, the results confirm that RH-derived RE-doped nanosilica can convert high-energy UV photons into visible emissions spanning blue, white, red, and orange. The broad excitation window (220–400 nm) overlaps with UV–near-UV LED sources and the solar UV spectrum, making these phosphors ideal candidates for LDS layers in photovoltaic modules [52]. Enhanced spectral response can improve silicon solar cell performance while simultaneously providing photostability against UV-induced degradation [53].

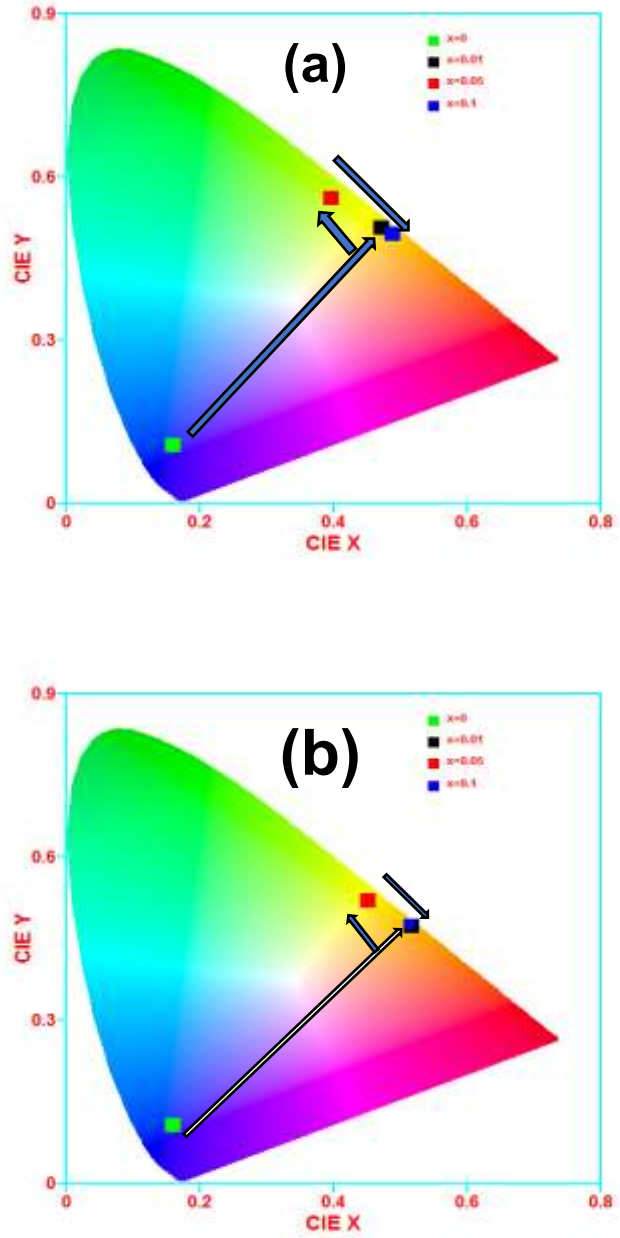

Figure 16: Chromaticity coordinate diagram of host (x=0) & RH-SiO_2: x Sm^{3+} (x=0.01, 0.05 & 0.1 molar ratios) excited at 365 nm (a), and RH-SiO_2: x Sm^{3+} (x=0.01, 0.05 & 0.1 molar ratios) excited at 400 nm (b

5.0 Conclusion and Recommendations

5.1 Conclusion

This study demonstrates that rare-earth-doped nanosilica derived from rice husk offers a viable pathway for producing high-performance luminescent materials through a sustainable, low-cost synthesis route. The structural, morphological, and optical analyses confirmed that the dual-acid-treated and thermally optimized nanosilica provides a stable amorphous host capable of effectively accommodating rare-earth dopants. The resulting materials exhibit strong, tunable photoluminescence suitable for luminescent downshifting applications.

The findings further reveal that dopant concentration has a strong influence on emission profiles, enabling customizable spectral responses for specific photonic applications. Overall, the successful conversion of rice husk into functional nanosilica supports environmental sustainability, promotes waste-to-wealth innovation, and offers promising opportunities for enhancing photovoltaic efficiency.

5.2 Recommendations

i Optimize Doping Strategies: Future work should explore co-doping and concentration-controlled approaches to achieve higher emission intensities and mitigate quenching effects.
ii Enhance Surface Functionalization: Modifying the nanosilica surface with tailored chemical groups could improve energy transfer pathways and overall photoluminescent efficiency.
iii Advance Photovoltaic Integration: Further studies should focus on integrating these materials as luminescent downshifting layers in real photovoltaic devices to quantify efficiency gains.
iv Scale-Up and Industrial Translation: The synthesis method should be scaled and evaluated for manufacturing feasibility, cost efficiency, and compatibility with commercial optical-grade coatings.
v Broaden Application Areas: Beyond photovoltaics, exploration into LEDs, optical sensors, and photonic coatings is recommended to fully exploit the multifunctional potential of the doped nanosilica.

Declarations

Declaration of Originality

The authors affirm that the manuscript titled “Synthesis and Characterization of Rare-Earth-Doped Nanosilica from Rice Husk for Potential Luminescent Downshifting Applications in Photovoltaics” contains original research that has not been published previously and is not under consideration elsewhere. The work is submitted exclusively to *Frontiers in Applied Physics, Materials Science and Nanotechnology*.

Author Contributions

Celestine Mbakaan conceived and designed the study, supervised the experimental work, conducted data interpretation, and prepared the manuscript. All authors reviewed and approved the final version and agree to be accountable for all aspects of the work.

Conflict of Interest Statement

The authors declare that no commercial or financial conflicts of interest exist in relation to this work.

Funding Statement

This work was fully supported by the Tertiary Education Trust Fund (TETFund), Nigeria, through the Institutional-Based Research (IBR) Grant.
The funding agency had no role in the study design, data analysis, interpretation of results, or the decision to submit the manuscript for publication.

Ethical Approval

This study involved no human participants or animal subjects. All laboratory activities were conducted according to institutional and national standards for safe scientific research.

Data Availability Statement

The datasets generated and analyzed during the current study are available from the corresponding author upon reasonable request. Additional supplementary data can be provided to reviewers if required.

Acknowledgements

The authors gratefully acknowledge the Tertiary Education Trust Fund (TETFund), Nigeria, for providing financial support through the Institutional-Based Research (IBR) Grant that enabled the successful execution of this project.

Permission to Publish

The author has approved the final manuscript and consents to its submission and publication in *Frontiers in Applied Physics, Materials Science and Nanotechnology*.

References

[1] H. Hoppe, "Recent developments in the field of inorganic phosphors," *Angew. Chem. Int. Ed.*, vol. 48, no. 20, pp. 3572–3582, 2009. doi:10.1002/anie.. 200804278.

[2] A. Birkel, K. A. Denault, N. C. George, and R. Seshadri, "Advanced inorganic materials for solid-state lighting," *Mater. Matters*, vol. 7, no. 2, pp. 22–27, 2012 .

[3] W. H. Green, K. P. Le, J. Grey, T. T. Au, and M. J. Sailor, "White phosphors from a silicate-carboxylate sol-gel precursor that lack metal activator ions," *Science*, vol. 276, no. 5320, pp. 1826–1828, 1997 .

[4] S. Nobre, X. Cattoen, R. A. S. Ferreira, M. W. C. Man, and L. D. Carlos, "Efficient spectrally dynamic blue-to-green emission of bipyridine–based bridged silsesquioxanes for solid-state lighting," *Phys. Status Solidi RRL*, vol. 4, pp. 55–57, 2010 .

[5] M. Narisawa et al., "Long-lived photoluminescence in amorphous Si–O–C(–H) ceramics derived from polysiloxanes," *J. Am. Ceram. Soc.*, vol. 95, pp. 3935–3940, 2012 .

[6] Z. Wang et al., "Luminescence mechanism of carbon incorporated silica nanoparticles derived from rice husk biomass," *Ind. Eng. Chem. Res.*, vol. 56, pp. 5906–5914, 2017 .

[7] Z. Wei et al., "Synthesis of green phosphors from highly active amorphous silica derived from rice husks," *J. Mater. Sci.*, 2017. doi:10.1007/s10853-017-1637-x .

[8] R. Bryant et al., "Genetic variation and association mapping of silica concentration in rice hulls using a germplasm collection," *Genetica*, vol. 139, no. 11–12, pp. 1383–1398, 2011 .

[9] G. Habeeb and M. Fayyadh, "Rice husk ash concrete: the effect of RHA average particle size on mechanical properties and drying shrinkage," *Aust. J. Basic Appl. Sci.*, vol. 3, no. 3, pp. 1616–1622, 2009 .

[10] S. Park, S.-R. Lim, Y.-S. Yun, and J.-M. Park, "Development of a new Cr(VI)-biosorbent from agricultural biowaste," *Bioresour. Technol.*, vol. 99, no. 18, pp. 8810–8818, 2008 .

[11] J. Yu, J. Zhang, J. He, Z. Liu, and Z. Yu, "Combinations of mild physical or chemical pretreatment with biological pretreatment for enzymatic hydrolysis of rice hull," *Bioresour. Technol.*, vol. 100, no. 2, pp. 903–908, 2009 .

[12] W. Wang et al., "Harvesting silica nanoparticles from rice husks," *J. Nanopart. Res.*, vol. 13, no. 12, pp. 6981–6990, 2011 .

[13] W. Wang et al., "Silica nanoparticles and frameworks from rice husk biomass," *ACS Appl. Mater. Interfaces*, vol. 4, no. 2, pp. 977–981, 2012 .

[14] Z. Wang et al., "Large-scale and controllable synthesis of graphene quantum dots from rice husk biomass: A comprehensive utilization strategy," *ACS Appl. Mater. Interfaces*, vol. 8, no. 2, pp. 1434–1439, 2016 .

[15] N. Yalcin and V. Sevinc, "Studies on silica obtained from rice husk," *Ceram. Int.*, vol. 27, no. 2, pp. 219–224, 2001 .

[16] V. M. Gun'ko et al., "Structural, textural, and adsorption characteristics of nanosilica mechanochemically activated in different media," *J. Colloid Interface Sci.*, vol. 355, no. 2, pp. 300–311, 2011 .

[17] C. D. S. Brites et al., "Metal-free highly luminescent silica nanoparticles," *Langmuir*, vol. 28, no. 12, pp. 8190–8196, 2012 .

[18] J. Slowing, B. Trewyn, S. Gin, and V. S.-Y. Lin, "Mesoporous silica nanoparticles for drug delivery and biosensing applications," *Adv. Funct. Mater.*, vol. 17, no. 8, pp. 1225–1236, 2007 .

[19] A. Alshatwi, J. Athinarayanan, and V. Periasamy, "Biocompatibility assessment of rice husk-derived biogenic silica nanoparticles for biomedical applications," *Mater. Sci. Eng. C*, vol. 47, pp. 8–16, 2015 .

[20] V. Bansal, A. Ahmad, and M. Sastry, "Fungus-mediated biotransformation of amorphous silica in rice husk to nanocrystalline silica," *J. Am. Chem. Soc.*, vol. 128, no. 43, pp. 14059–14066, 2006 .

[21] M. Bhagiyalakshmi, L. J. Yun, R. Anuradha, and H. T. Jang, "Utilization of rice husk ash as silica source for the synthesis of mesoporous silicas and their application to CO_2 adsorption," *J. Hazard. Mater.*, vol. 175, no. 1–3, pp. 928–938, 2010 .

[22] N. Zemnukhova et al., "Properties of amorphous silica produced from rice and oat processing waste," *Inorg. Mater.*, vol. 42, no. 1, pp. 24–29, 2006 .

[23] K. Binnemans, "Interpretation of europium(III) spectra," *Coord. Chem. Rev.*, vol. 295, pp. 1–45, 2015. doi:10.1016/j.ccr.2015.02.015.

[24] J. Gong et al., "Synthesis and luminescence properties of monodisperse SiO_2@SiO_2:Eu^{2+} microspheres," *Opt. Mater.*, vol. 37, pp. 583–588, 2014.

[25] G. Gutzov et al., "Preparation and optical properties of samarium-doped sol-gel materials," *J. Non-Cryst. Solids*, vol. 354, pp. 3438–3442, 2008.

[26] ISO, *Determination of the Specific Surface Area of Solids by Gas Adsorption — BET Method*, 2nd ed., BS ISO 9277, 2010.

[27] S. Bonacchi et al., "Luminescent silica nanoparticles: Extending the frontiers of brightness," *Angew. Chem. Int. Ed.*, vol. 50, no. 18, pp. 4056–4066, 2011.

[28] J. Herná, R. L. Lee, and J. Romero, "Calculating correlated color temperatures across the entire gamut of daylight and skylight chromaticities," *Appl. Opt.*, vol. 38, pp. 0–6, 1999.

[29] J. Umeda and K. Kondoh, "Process parameters optimization in preparing high-purity amorphous silica originated from rice husks," *Mater. Trans.*, vol. 48, no. 12, pp. 3095–3100, 2007.

[30] W. Wang et al., "Harvesting silica nanoparticles from rice husks," *J. Nanopart. Res.*, vol. 13, no. 12, pp. 6981–6990, 2011.

[31] Z. Wang et al., "Silica nanoparticles and frameworks from rice husk biomass," *ACS Appl. Mater. Interfaces*, vol. 4, no. 2, pp. 977–981, 2012.

[32] M. Bhagiyalakshmi, L. J. Yun, R. Anuradha, and H. T. Jang, "Utilization of rice husk ash as silica source for mesoporous silicas and CO_2 adsorption," *J. Hazard. Mater.*, vol. 175, no. 1–3, pp. 928–938, 2010.

[33] P. M. Aneesh, M. K. Krishna, and M. K. Jayaraj, "Hydrothermal synthesis and characterization of undoped and Eu-doped $ZnGa_2O_4$ nanoparticles," *Solid State Ionics*, vol. 156, no. 3, pp. K33–K38, 2009.

[34] L. Vaccaro et al., "Defect-related visible luminescence of silica nanoparticles," *Phys. Status Solidi C*, vol. 10, no. 1, pp. 1–4, 2013.

[35] L. Vaccaro et al., "Bright luminescence in silica nanoparticles," *J. Phys. Chem. C*, vol. 115, no. 41, pp. 19476–19481, 2011.

[36] H. Lin et al., "Blue photoluminescence from amorphous silica nanoparticles," *J. Appl. Phys.*, vol. 116, no. 23, p. 233104, 2014.

[37] J. Gong et al., "Synthesis and luminescence properties of monodisperse silica microspheres," *Opt. Mater.*, vol. 37, pp. 583–588, 2014.

[38] W. Wang et al., "Silica nanoparticles and frameworks from rice husk biomass," *ACS Appl. Mater. Interfaces*, vol. 4, no. 2, pp. 977–981, 2012.

[39] M. Bhagiyalakshmi et al., "Utilization of rice husk ash as silica source for mesoporous silicas and CO_2 adsorption," *J. Hazard. Mater.*, vol. 175, no. 1–3, pp. 928–938, 2010.

[40] K. Binnemans, "Interpretation of europium (III) spectra," *Coord. Chem. Rev.*, vol. 295, pp. 1–45, 2015.

[41] G. Gutzov et al., "Preparation and optical properties of samarium-doped sol–gel materials," *J. Non-Cryst. Solids*, vol. 354, no. 34, pp. 3438–3442, 2008.

[42] S. Bonacchi et al., "Luminescent silica nanoparticles: Extending the frontiers of brightness," *Angew. Chem. Int. Ed.*, vol. 50, pp. 4056–4066, 2011.

[43] Z. Wei et al., "Synthesis of green phosphors from highly active amorphous silica derived from rice husks," *J. Mater. Sci.*, vol. 52, no. 14, pp. 8378–8388, 2017.

[44] V. Gun'ko et al., "Structural, textural, and adsorption characteristics of nanosilica mechanochemically activated in different media," *J. Colloid Interface Sci.*, vol. 355, no. 2, pp. 300–311, 2011.

[45] C. D. S. Brites et al., "Metal-free highly luminescent silica nanoparticles," *Langmuir*, vol. 28, no. 12, pp. 8190–8196, 2012.

[46] M. Ishikawa et al., "White luminescence from rice husk-derived silica," *Appl. Phys. Lett.*, vol. 98, no. 24, p. 241904, 2011.

[47] A. Abbass, H. Swart, and R. Kroon, "White luminescence from sol–gel silica doped with silver," *J. Sol-Gel Sci. Technol.*, vol. 76, no. 3, pp. 708–714, 2015.

[48] Z. Wang et al., "Luminescence mechanism of carbon-incorporated silica nanoparticles derived from rice husk biomass," *Ind. Eng. Chem. Res.*, vol. 56, no. 20, pp. 5906–5914, 2017.

[49] M. Vishwakarma, R. Rai, and D. Kumar, "Optical properties of Dy^{3+}-doped phosphors for white light emission," *J. Lumin.*, vol. 167, pp. 275–282, 2015.

[50] A. Ahemen and R. Dejene, "Eu^{3+}-activated phosphors: Judd–Ofelt analysis and red emission applications," *Opt. Mater.*, vol. 75, pp. 66–73, 2018.

[51] G. Kaur et al., "Concentration quenching in Sm^{3+}-doped phosphors," *J. Mater. Sci. Mater. Electron.*, vol. 27, no. 6, pp. 6246–6252, 2016.

[52] J. Chen et al., "Luminescent downshifting layers for solar cells: fundamentals and applications," *Prog. Photovolt. Res. Appl.*, vol. 25, pp. 604–626, 2017.

[53] J. Zhang et al., "Spectral management for photovoltaics: luminescent down-shifting and upconversion," *Energy Environ. Sci.*, vol. 11, pp. 1219–1249, 2018.

[54] Y. Zhang, J. Wang, L. Liu, and K. Xu, "Enhanced down-shifting photoluminescence in Eu^{3+}-doped SiO_2 thin films for photovoltaic applications," *Solar Energy Materials and Solar Cells*, vol. 260, p. 112361, 2023.

[55] H. Li, X. Zhao, and P. Yang, "Synthesis and characterization of Dy^{3+}-doped silica nanophosphors derived from rice husk for eco-friendly luminescent coatings," *Journal of Luminescence*, vol. 259, p. 120894, 2023.

[56] R. Gupta, S. Patel, and T. Ramesh, "Sustainable synthesis of mesoporous nanosilica from rice husk ash for energy and optical applications," *Materials Today: Proceedings*, vol. 74, pp. 134–142, 2024.

[57] M. N. Al-Mamun, A. M. Yousuf, and F. Ahmed, "Photoluminescence and energy transfer mechanisms in rare-earth-doped silica nanomaterials," *Ceramics International*, vol. 50, no. 1, pp. 101–112, 2024.

[58] D. Kim, Y. Park, and S. Lee, "Spectral conversion and UV stability of Eu^{3+}/Dy^{3+} co-doped silica nanoparticles for improved photovoltaic response," *Optical Materials Express*, vol. 13, no. 7, pp. 2218–2231, 2023.

[59] E. R. Adegbite, I. O. Afolayan, and C. N. Obasi, "Rice husk-derived nanosilica as a sustainable host for rare-earth photoluminescent systems," *Heliyon*, vol. 10, no. 4, p. e26845, 2024.